Earth Sciences
2025, Vol. 14, No. 1, pp. 33-48
https://doi.org/10.11648/j.earth.20251401.13

Research Article

On the Relationships Between the Main Parameters of an Earthquake and Its Actual Consequences on the Earth's Surface the Magnitude and Seismic Moment of Earthquake

Eduard Khachiyan[1, 2, *]

[1]Scientific Department, National University of Architecture and Construction of Armenia, Yerevan, Armenia
[2]Institute of Geological Sciences, National Academy of Sciences of the Republic of Armenia, Yerevan, Armenia

Abstract

Based on new research, the article presents a formula for determining the potential energy of an earthquake with incorporation of seismic moment and displacement angle values. This formula is new compared to the one derived by the author earlier. The mechanical interpretation of the new formula is provided. Much effort is devoted to determining the values of "stress relief" during strong earthquakes. A formula is derived for determining the values of "stress relief" based on shear modulus and ultimate shear strain of the soil stratum at the epicenters of 44 earthquakes. Also, a methodology is offered to determine energy values of earthquakes with complex structures of surface rupture, as well as areas of deformation zones on Earth's surface and areas of strong earthquake aftershocks' locations. New formulas are derived for determining such areas and a comparative analysis is provided with similar formulas by K. Kasahara and T. Dambara.

Keywords

Earthquake Energy, Seismic Moment, Displacement Angle, Stress Relief, Deformation Areas and Aftershock Locations, Empirical Dependencies

1. Introduction

In 2013-2022 Science Publishing Group's journal Earth Sciences published the author's four articles [1-4] on some of the new undertakings in applied seismology. In the ensuing years the author developed some major additions to the mentioned articles, which are shared herein.

2. A New Formula for the Value of Earthquake's Energy

This part is an addition to the article Method for Determining the Potential Strain Energy Stored in the Earth before a Large Earthquake. Science Publishing Group, Earth Sciences, vol. 2, issue 2, 2013 pp 47-57. In this article [1], based on many assumptions the following main formula was derived for the potential energy of an earthquake E_d, (see Figures 1, 2)

$$E_d = \frac{\pi^2}{32}\frac{LhG}{R}\overline{u}^2 \quad (1)$$

*Corresponding author: edkhach@sci.am (Eduard Khachiyan)

Received: 7 January 2025; **Accepted:** 23 January 2025; **Published:** 26 February 2025

where: $\overline{u}$ is the earthquake's mean slip [8], L is the rupture length at the Earth's surface, h rupture depth, G is the shear modulus of the ground rocks, and R is the length of the deformed medium (Figure 2) depending on the mean value of slip after the earthquake (in meters), expressed as:

$$R = 5(\overline{u} + 3) \cdot 10^3 \quad (2)$$

The main assumption is that the mean value of slip after the rupture occurs is equal to the sum of the two halves of the medium's long-lasting static deformation $u_0/2$ and the main function of the movement perpendicular to the rupture direction is as follows (Figure 2c):

$$U(x) = \frac{\overline{u}}{2} cos \frac{\pi x}{2R} \quad (3)$$

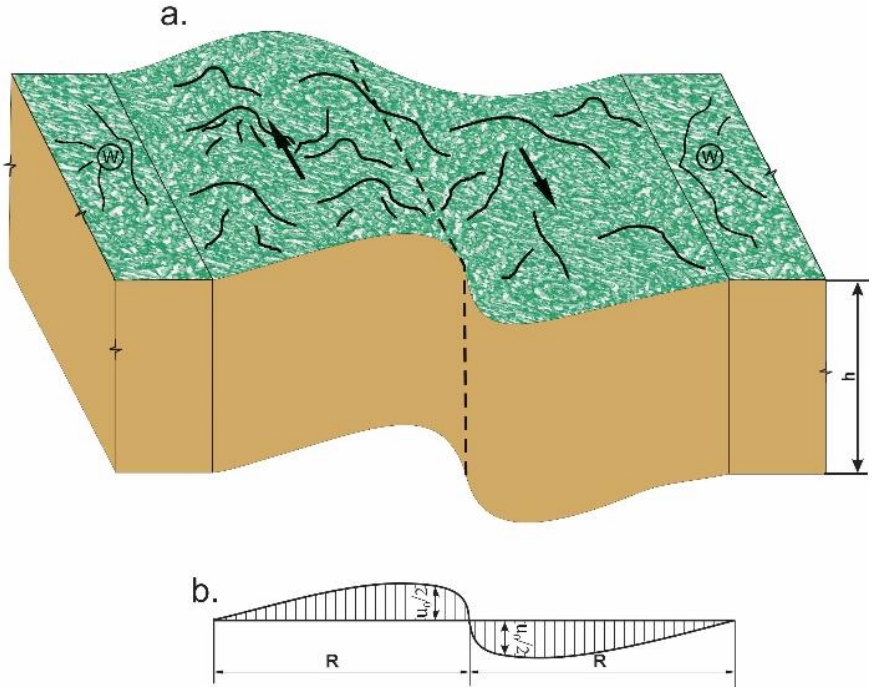

Figure 1. *Schematic illustration of a slow and lengthy deformation of the medium over a long period of an earthquake maturing, a. deformed condition of the medium before development of the rupture, b. distribution of displacements of the medium in the direction perpendicular to the rupture before the earthquake, h is the depth of the future rupture, $u/2$ is static deformations of blocks the moment rupture occurs, R is length of the deformation area perpendicular to the rupture, W are regions suggested as not deformed by maturing earthquakes because of relatively small deformations compared to the u at the rupture. Arrows show directions of slow slips of blocks, dashed line shows the line of future rupture.*

The formula of deformation's potential energy (1) can be interpreted differently from the perspective of mechanics. Indeed, it is known that determining a registered earthquake's magnitude is marred difficulties related to the sensitivities of seismographs vis-à-vis the Wood-Anderson seismograph, especially for very weak and very strong earthquakes. In this relation, it was thought that earthquake strength can be measured directly by the earthquake focus parameters at Earth's surface. As it was noted in [1], in the process of earthquake, in some region of Earth's crust a sudden rupture of rocks occurs along a plane with certain area and relative slip. Obviously, the larger the rupture area and relative slip, the stronger the earthquake. It is considered that the rupture area is in the form of a very thin plate with lateral dimensions of L and h, and thickness of b, as shown on Figure 3. Before rupture, the tangent forces τ_{xy} make its two sides move relative to each other at a value of u. Since before the rupture this plate is in the state of equilibrium, it can be assumed that a pair of forces P apply on its sides with the moment of $M_0 = PL$ which is called seismic moment of an earthquake. It follows from Figure 3 that the following ratios apply:

$$\gamma \frac{b}{2} = \frac{u}{2}, \tau = \gamma G.$$

Thus, the seismic moment of an earthquake is the product of three values of an occurred earthquake: rupture area, shear modulus and relative slip of the ruptured parts, which is usually measured in dyn×cm. The main point is that the value of the seismic moment of an earthquake can be calculated only for earthquakes that caused a rupture at Earth's surface, i.e. for the strongest earthquakes referred to in our articles [1-4].

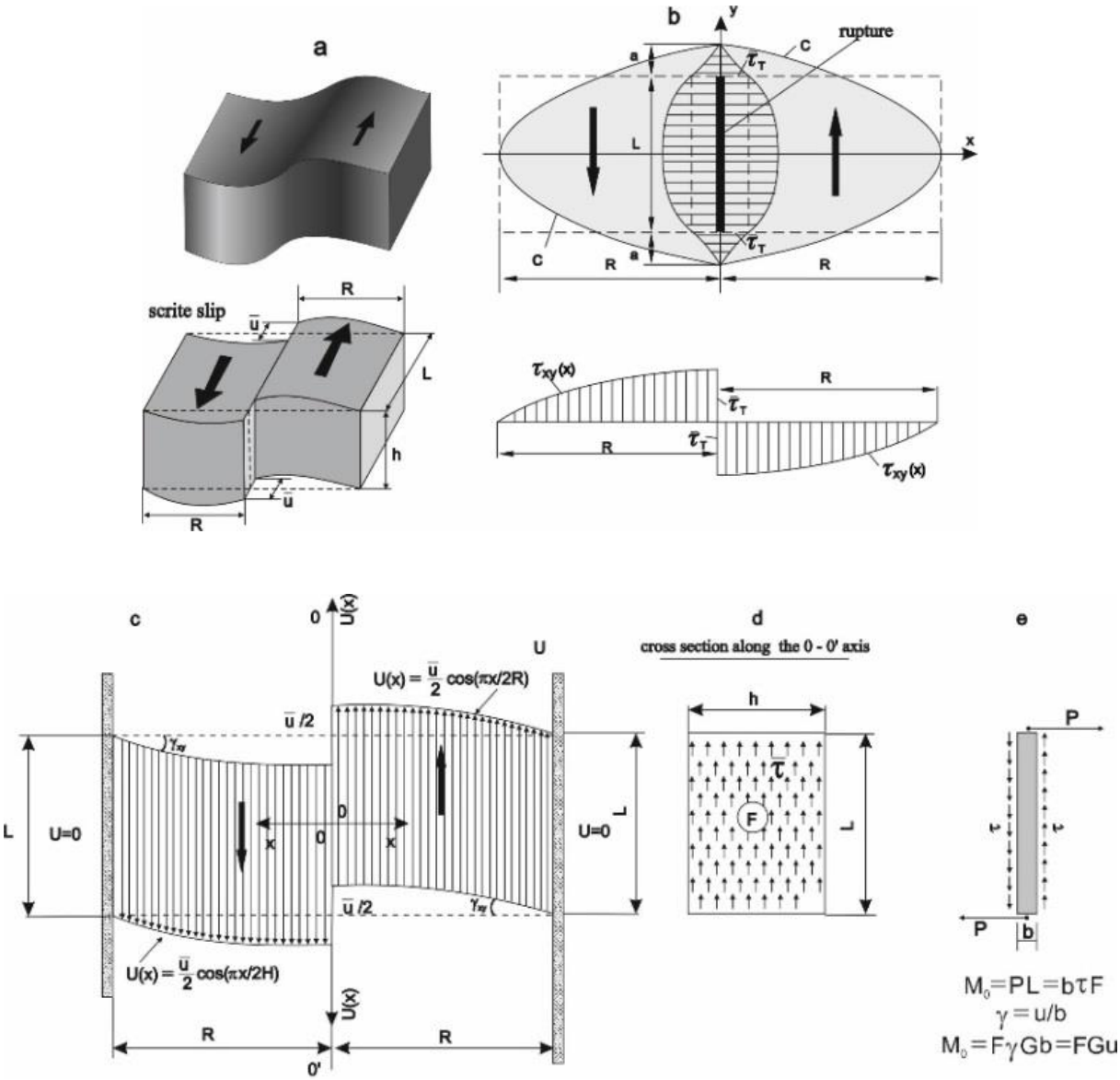

Figure 2. *Schematic illustration of the medium stress condition a-before formation of the rupture, b-after formation of the rupture, c-equivalent areas of stress conditions, d-distribution of shear stresses, (ɑlim -limit resistance of rocks), e-interpretation of the physical essence of the seismic moment.*

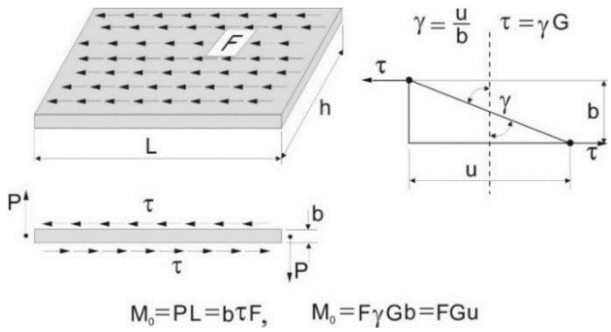

Figure 3. *The mechanism of the rupturing process and illustration of the seismic moment's occurrence [5, 6].*

Therefore (Figure 3):

$$M_0 = PL = F\gamma Gb = F\gamma G\frac{u}{\gamma} = FGu \tag{4}$$

This important concept was first introduced in seismology by K. Aki [6], who calculated its value first time for the Niigata Earthquake of June 16, 1964 with magnitude $M = 7.5$ and $M_0 = 273 \cdot 10^{25}\, dyn \cdot cm$.

Now let us get back to the main formula for the energy of an earthquake (1). In applied problems of material mechanics [7] when determining post and beam deflections from slip, the shear rigidity is assumed FG/k', where F is the cross-sectional area of an element, G is the shear modulus, k' is called form coefficient of slip and for a rectangular

cross-section $k' = 5/6 = 0.833$ [7]. Based on the above-mentioned, the formula (1) can be presented as a product of three parts, as follows:

$$E_d = \frac{LhG\bar{u}}{2} \cdot \frac{\bar{u}\pi}{2 \cdot 2R} \cdot \frac{\pi}{4k'} \quad (5)$$

It is easy to see that the first multiplier in (5) is the half of the value of seismic moment of an earthquake, i.e. $M_0/2$, while the second multiplier in (5) is the maximum value of the first order derivative γ_{xy} of the main movement function (3) $U(x)$ assumed in deducing the main formula for energy (1), at the end-part of a conditionally fixed beam with dimensions of $L \times h \times R$ (Figure 2b), i.e.:

$$\gamma_{xy} = \frac{dU(x)}{dx} = \frac{\bar{u}\pi}{2 \cdot 2R} \cdot sin\frac{\pi x}{2R}\Big|_{x=R} = \gamma_{xymax} = \gamma_{lim} = \frac{\bar{u}\pi}{2 \cdot 2R} \quad (6)$$

and finally, the third multiplier in (5) can be assumed to be $\pi/4k' \approx 1$.

Note that the movement function (3) we used in [1] satisfies the following four boundary conditions:

$$\text{for } x = 0\ U(x) = \frac{\bar{u}}{2},\ \frac{dU(x)}{dx} = 0$$

$$\text{for } x = R\ U(x) = 0,\ \frac{dU(x)}{dx} = \gamma_{xy}$$

Note that the angle γ_{xy} may not be equal to zero, since it expresses the value of the medium shear deformation in the adopted design scheme (Figure 2c).

No comprehensive results were achieved in an attempt to find an alternative displacement function $U(x)$. In [2], the following version of displacement function $U(x)$ was accepted:

$$U(x) = \frac{\tau_{lim}}{G}\frac{2R}{\pi}(sin\frac{\pi x}{2R} - 1), \quad (7)$$

Despite the fact that the function satisfies the boundary conditions (under $x = 0$ and $x = R$), and that based on the condition (Figure 2 c):

For $x = 0\ U(x) = -\frac{\bar{u}}{2}$ or $-\frac{\bar{u}}{2} = -\frac{\tau_{lim}}{G}\frac{2R}{\pi}$, it follows that:

$$\frac{\tau_{lim}}{G} = \gamma_{xylim} = \frac{\bar{u}}{2} \cdot \frac{\pi}{2R}$$

Which is the same result that can be derived from the formula (5):

$$\gamma_{xylim} = \frac{dU(x)}{dx}\Big|_{x=R} = \frac{\bar{u}\pi}{2 \cdot 2R} = \gamma_{lim},$$

But it does not meet one of the major conditions of the problem that at the point $x = R$, the derivative $\frac{dU(x)}{dx}$ cannot be equal to zero. Therefore, the only function $U(x)$, adopted in [1] that meets all the boundary and physical conditions is the equation (3).

This is also confirmed by the fact that the new formulas obtained in [1-3] for determining the values of the earthquake energy, ultimate shear strain of the ground, and, as it is shown below, the values of "stress relief", match the same obtained by other authors through geodetical methods.

Thus, the formula (1) for determining the value of the earthquake energy E_d can be presented in the following form:

$$E_d = \frac{M_0\gamma_{lim}}{2}. \quad (8)$$

This formula is similar to the one for deformation energy for bars and posts torsion, just with a difference that in case of the torsion instead of seismic moment M_0 the value of real torque M_{tor} is used, and instead of displacement angle γ_{xy},

$$E = \frac{M_{tor}\varphi}{2}. \quad (9)$$

torsion angle φ is used. That is quite explicable, since in torsion and in straight displacement only tangential strains are created. It has to be mentioned that according to the theory of elasticity, the tangential stresses in mutually perpendicular planes are equal to each other [6].

Table 1 shows the earthquake energy classes k_d, computed by the main formula (1) and the formula (8). The results indicate only insignificant differences.

Therefore, it can be stated that the earthquake energy E_d is the work of the earthquake's seismic moment M_0 on the entire space of the deformed medium, on both sides of the future rupture caused by the pending earthquake.

3. About "Stress Relief"

As mentioned above, the main function of the movement (3) was used in [1] to prove that the deformation energies for 44 earthquakes are equal when calculated by the method we developed and by the known formula of the Gutenberg–Richter law for the earthquake magnitude M_s. In parallel, formula (3) can be used to determine the ultimate shear strain and tangential stresses for any points of the deformed medium $0 \le x \le R$, based on the following formulas:

$$\tau_{xy} = G\gamma_{xy},\ \gamma_{xy} = \frac{dU(x)}{dx} = \frac{\bar{u}}{2}\frac{\pi}{2R}sin\frac{\pi x}{2R}. \quad (10)$$

The maximum value of γ_{xy}, which is also ultimate shear strain of the ground ($\gamma_{xymax} = \gamma_{lim}$), will be expressed as follows:

$$\gamma_{xymax} = \frac{\bar{u}}{2} \cdot \frac{\pi}{2R}. \quad (11)$$

Therefore, if $\overline{u}$ is the slip value at which ground rupture (earthquake) occurred, then the maximum value γ_{xymax} will be equal to the earthquake's ultimate shear strain γ_{lim} of the soil stratum with a thickness of *h*.

Considering formula (2), the γ_{lim} will turn into:

$$\gamma_{lim} = \frac{\pi}{2} \cdot \frac{\overline{u}}{\overline{u}+3} \cdot 10^{-4}. \quad (12)$$

Unlike the usual impacts, earthquakes cause shear deformations of not just a homogenous layer of a certain ground, but of a whole stratum with various soils with a large thickness which is equal to the earthquake focus depth. Hence, the actual value of the crust's shear strain can be determined only by the deformation parameters of the earthquake focus at the last stage before such earthquake occurs.

Considering that based on Table 1, the rupture length L for all studied earthquakes is larger than the length R, it can be assumed that during the static deformation process both prismatic spaces with dimensions L x h x R were subjected to slip, as it is shown on Figure 2 for the left-lateral slip (LL).

Since we presume that the value of slip $\overline{u}/2$ is also the ultimate static shear strain at which the rupture of the medium occurred, the maximum shear strain obtained through the formula (9) can be considered the ultimate slip deformation of the ground at the earthquake focus. On the other hand, Hooke's law implies the following:

$$\tau_{r.s.} = \gamma_{lim} G \quad (13)$$

which can be used to calculate also the values of "stress relief" $\tau_{r.s.}$ for the considered 44 earthquakes [8]. The penultimate column of Table 1 shows the ultimate shear strain values γ_{lim} for the rocks at the foci of all 44 earthquakes. The maximum values of ultimate strain reached 1.15 x 10^{-4} ($M = 8.0, u_{max} = 8$ m), the minimum value was 0.02 x 10^{-4} ($M = 5.6, u_{max} = 0.5$ m), and the mean value for the 44 earthquakes – $\bar{\gamma}_{\text{lim}} = 0.52 \times 10^{-4}$.

It is shown in [2] that these numbers are similar to the data by Tsuboi (1932), Rikitake (1979) [13], Kasahara (1981) [10], and Mogi (1985) [12] that were obtained for individual earthquakes by geodetic methods, which indirectly proves the sufficient credibility of the function (3).

The only additional important parameter of formula (12) is the value of earthquake slip $\overline{u}$, while the earthquake strength is not important. If an earthquake caused a slip, then certainly a rupture of medium occurred to the depth of h, with a length of L and an area of $F = Lh$. The larger the slip, the stronger the earthquake and the firmer is the layer with the height of h. As seen in Table 1, the maximum slip reached 14.6 m at $M = 7.9$, and the minimum slip is 0.1 m at $M = 5.6$. As it was shown in [2], the earthquake magnitude M and ultimate value γ_{lim} are related as follows:

$$10^4 \gamma_{lim} = 0.39M - 2.23. \quad (14)$$

As for stress relieves $\tau_{r.s.}$, it follows from the above-mentioned that formula (13) can be used to calculate the maximum value of the relieved tangential strain τ_{lim} before the earthquake. In seismology these are called "stress relief", based on the elastic-rebound theory of Reid.

Formula (13) implies that the value of stress relieves is directly proportional to shear modulus G of the rocks in the Earth's crust. In seismology and geotechnology, for the upper, near-surface rocks G value is accepted as $G = (3 \div 5) \cdot 10^5$kg/cm^2. Assuming that $G = 5 \cdot 10^5$ kg/cm^2, the last column of Table 1 shows the stress relief values for 44 earthquakes, which are in the range from 2 to 57.5 kg/cm^2. The stronger the earthquake, the higher the stress relief values.

Figure 4(a) shows dependence of stress relief $\tau_{r.s.}$ on magnitude M and Figure 4(b) on mean slip $\overline{u}$. Our research shows that for the 44 selected earthquakes, mean slip values $\overline{u}$ are 1.95-2.08 times smaller than the maximum slip values u_{max} (Figure 5).

Table 1. *Earthquake parameters [8] and values of energy class k_d, ultimate shear strain γ_{lim} and stress relief $\tau_{r.s.}$*

No.	Country	Earthquake location	Date of earthquake occurrence	Type of slip	Earthquake magnitude M_s	Rupture length L, [km]	Rupture depth h, [km]	Maximum slip u_{max}, [m]
1	USA	Fort Tejon	09.01.1857	RL	8.3	297	12	9.4
2	USA	Owens Valley	26.03.1872	RL-N	8	108	15	11
3	Japan	Nobi	27.10.1891	LL	8	80	15	8
4	Japan	Rikuu	31.08.1896	R	7.2	40	21	4.4
5	USA	San Francisco	1/13/1906	RL	7.8	432	12	6.1
6	USA	Pleasant Valley	10/3/1915	N	7.6	62	15	5.8
7	China	Kansy	12/16/1920	LL	8.5	220	20	10

No.	Country	Earthquake location	Date of earthquake occurrence	Type of slip	Earthquake magnitude M_s	Rupture length L, [km]	Rupture depth h, [km]	Maximum slip u_{max}, [m]
8	Japan	North Izu	11/25/1930	LL- R	7.3	35	12	3.8
9	China	Kehetuohai	8/10/1931	RL	7.9	180	20	14.6
10	Turkey	Erzincan	12/26/1939	RL	7.8	360	20	7.5
11	USA	Imperial Valley	5/19/1940	RL	7.2	60	11	5.9
12	China	Damxung	11/18/1951	RL	8	200	10	12
13	USA	Dixie Valley	12/16/1954	RL-R	6.8	45	14	3.8
14	Turkey	Abant	5/26/1957	RL	7	40	8	1.65
15	Mongolia	Gobi-Altai	12/4/1957	LL	7.9	300	20	9.6
16	USA	Hebgen Lake	8/18/1959	N	7.6	45	17	6.1
17	Iran	Dasht-e-Bayaz	8/31/1968	LL	7.1	110	20	5.2
18	Turkey	Gediz	3/28/1970	N	7.1	63	17	2.8
19	USA	San Fernando	2/9/1971	R-LL	6.5	17	14	2.5
20	China	Luhuo	2/6/1973	LL	7.3	110	13	3.6
21	Guatemala	Motagua	2/4/1976	LL	7.5	257	13	3.4
22	Turkey	Caldiran	11/24/1976	RL	7.3	90	18	3.5
23	Iran	Bob-Tangol	12/19/1977	RL	5.8	14	12	0.3
24	Greece	Thessaloniki	6/20/1978	N	6.4	28	14	0.22
25	Iran	Tabas-e-Colshan	9/16/1978	R	7.5	74	22	3
26	USA	Homestead Valley	3/15/1979	RL	5.6	6	4	0.1
27	Australia	Cadoux	6/2/1979	R	6.1	16	6	1.5
28	USA	El Centro	10/15/1979	RL	6.7	51	12	0.8
29	Iran	Koli	11/27/1979	LL-R	7.1	75	22	3.9
30	Algeria	El Asman	10/10/1980	R	7.3	55	15	6.5
31	Italy	South Apennines	11/23/1980	N	6.9	60	15	1.15
32	Greece	Corinth	2/25/1981	N	6.4	19	16	1.5
33	Greece	Corinth	3/4/1981	N	6.4	26	18	1.1
34	USA	Borah Peak	10/28/1983	N-LL	7.3	33	20	2.7
35	Algeria	Constantine	10/27/1985	LL	5.9	21	13	0.12
36	Australia	Marryat Creek	3/30/1986	R-LL	5.8	13	3	1.3
37	Greece	Kalamata	9/13/1986	N	5.8	15	14	0.18
38	New Zealand	Edgecumbe	3/2/1987	N	6.6	32	14	2.9
39	USA	Superstition Hills	11/24/1987	RL	6.6	30	11	0.92
40	Australia	Tennant Greek	1/22/1988	R	6.3	13	9	1.3
41	China	Lancand Gengma	11/6/1988	RL	7.3	80	20	1.5
42	Armenia	Spitak	12/7/1988	R-RL	6.8	38	11	2
43	Canada	Ungava	12/25/1989	R	6.3	10	5	2
44	USA	Landers	6/28/1992	RL	7.6	62	12	6

Table 1. *Continued.*

No.	Mean slip $\overline{u}$, [m]	Seismic moment $M_o x10^{-26}$, [dyne*cm]	Value of R from (2), [km]	Energy classes k_d (1)	Energy classes k_d (8)	Ultimate shear strain from (12) $\gamma_{\lim}$ x 104	Stress relief $\tau_{r.s.}$, kg/cm^2 $G = 5x10^5$ kg/cm^2
1	6.4	114.0	47	16.68	16.79	1.07	53.5
2	6	48.60	45	16.30	16.41	1.05	52.5
3	5.04	30.24	40.25	16.06	16.17	0.98	49
4	2.59	10.88	27.95	15.49	15.60	0.73	36.5
5	3.3	85.54	31.5	16.44	16.54	0.82	41
6	2	9.300	25	15.36	15.47	0.63	31.5
7	7.25	159.5	51.25	16.84	16.95	1.11	55.5
8	2.9	6.090	29.5	15.26	15.37	0.77	38.5
9	7.38	132.8	51.9	16.76	16.87	1.12	56
10	1.85	66.60	24.25	16.19	16.30	0.60	30
11	1.5	4.950	22.5	15.01	15.11	0.52	26
12	8	80.00	65	16.55	16.66	1.15	57.5
13	2.1	6.615	25.5	15.22	15.33	0.65	32.5
14	0.55	0.880	17.75	13.92	14.02	0.24	12
15	6.54	196.2	47.7	16.92	17.03	1.08	54
16	2.14	8.186	25.7	15.32	15.42	0.65	32.5
17	2.3	25.30	26.5	15.83	15.93	0.68	34
18	0.86	4.605	19.3	14.80	14.91	0.35	17.5
19	1.5	1.785	22.5	14.56	14.67	0.52	26
20	1.3	9.295	21.5	15.24	15.34	0.47	23.5
21	2.6	43.43	28	16.09	16.20	0.73	36.5
22	2.05	16.61	25.25	15.62	15.73	0.64	32
23	0.12	0.101	15.6	12.38	12.48	0.06	3
24	0.08	0.157	15.4	12.40	12.50	0.04	2
25	1.5	12.21	22.5	15.39	15.50	0.52	26
26	0.05	0.006	15.25	10.78	10.95	0.03	1.5
27	0.5	0.240	17.5	13.32	13.42	0.22	11
28	0.18	0.551	15.9	13.28	13.39	0.09	4.5
29	1.2	9.900	21	15.24	15.35	0.45	22.5
30	1.54	6.353	22.7	15.12	15.23	0.53	26.5
31	0.64	2.880	18.2	14.49	14.61	0.28	14
32	0.6	0.912	18	13.97	14.07	0.26	13
33	0.6	1.404	18	14.16	14.26	0.26	13
34	0.8	2.640	19	14.53	14.64	0.33	16.5
35	0.1	0.137	15.5	12.43	12.53	0.05	2.5
36	0.5	0.098	17.5	12.93	13.03	0.22	11

No.	Mean slip $\overline{u}$, [m]	Seismic moment $M_o x10^{-26}$, [dyne*cm]	Value of R from (2), [km]	Energy classes k_d (1)	Energy classes k_d (8)	Ultimate shear strain from (12) $\gamma_{\lim}$ x 104	Stress relief $\tau_{r.s.}$, kg/cm^2 $G = 5x10^5$ kg/cm^2
37	0.15	0.158	15.75	12.66	12.74	0.07	3.5
38	1.7	3.808	23.5	14.93	15.04	0.57	28.5
39	0.54	0.891	17.5	13.92	14.03	0.24	12
40	0.63	0.369	18.15	13.59	13.70	0.27	13.5
41	0.7	5.600	18.5	14.81	14.92	0.30	15
42	1.22	2.550	21.1	14.65	14.76	0.45	22.5
43	0.8	0.200	19	13.41	13.52	0.33	16.5
44	2.95	10.97	29.75	15.52	15.63	0.78	39

Hence, the values of stress relief $\tau_{r.s}$ on rupture middle areas will be about twice as high, so will reach from 4 to 115 kg/cm^2. According to Brune [5], stress relief values $\tau_{\lim}$ usually are in the range of 50-100 bar (kg/cm^2), with some as low as a few bars and some others as high as a few hundredbars. For the San Francisco earthquake of 1906 ($M = 7.8$), the stress relief value was estimated by geodetic methods to be 130 bars.

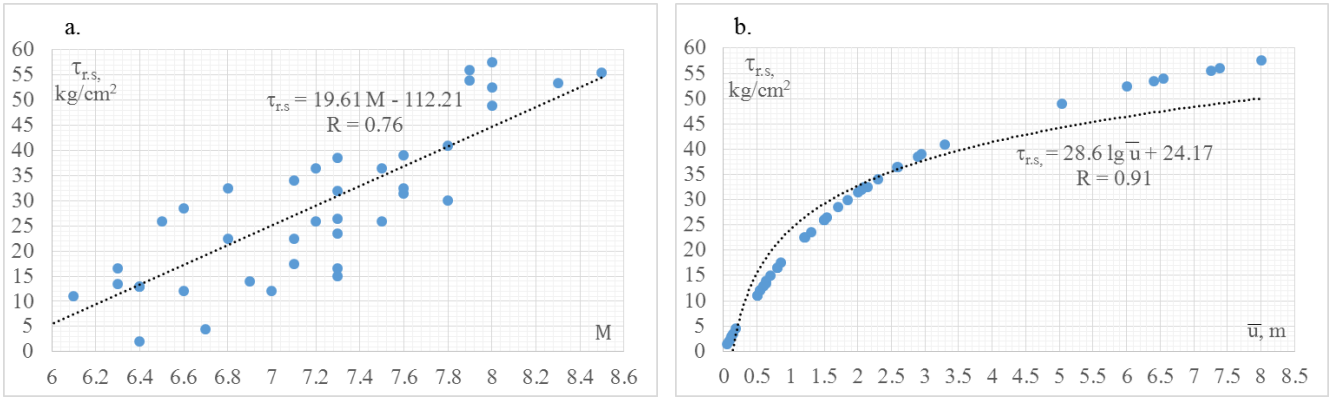

Figure 4. *Dependence of stress relief values $\tau_{r.s.}$ on: (a) magnitude M, and (b) on mean slip $\overline{u}$.*

As can be seen the stress relief values calculated by the formula (12) depend not only on the shear strain of the rocks, but also their shear modulus G. In [4] we have shown that for actual ground beddings with a depth of 30 m (andesite-basalt rocks of Armenia) of seismic Category I ($v_s = 2895$m/sec), based on synthetic accelerograms of earthquakes with magnitudes of 7.0, 8.0 and 9.0, at the bedding's base level (depth of 30 m) the design values of γ_{xy} reach $\gamma_{xy} = 0.5 \cdot 10^{-4}$, $0.89 \cdot 10^{-4}$ and $1.28 \cdot 10^{-4}$, respectively, while the stress relief values at $G = 5 \cdot 10^5$kg/cm^2 reach 25 kg/cm^2 at M = 7.0, 44 kg/cm^2 at M = 8.0, and 64 kg/cm^2 at M = 9.0.

Based on the commonly accepted view, the physical and mechanical characteristics of the deep rock layers undergo compression forces twice as high or even higher than the similar near-surface layers and assuming that $G = 2 \times 5 \times 105$ kg/cm^2, the values of maximal tangential strains would reach 50, 90, and 130 kg/cm^2 for $M = 7.0, 8.0, 9.0$, respectively.

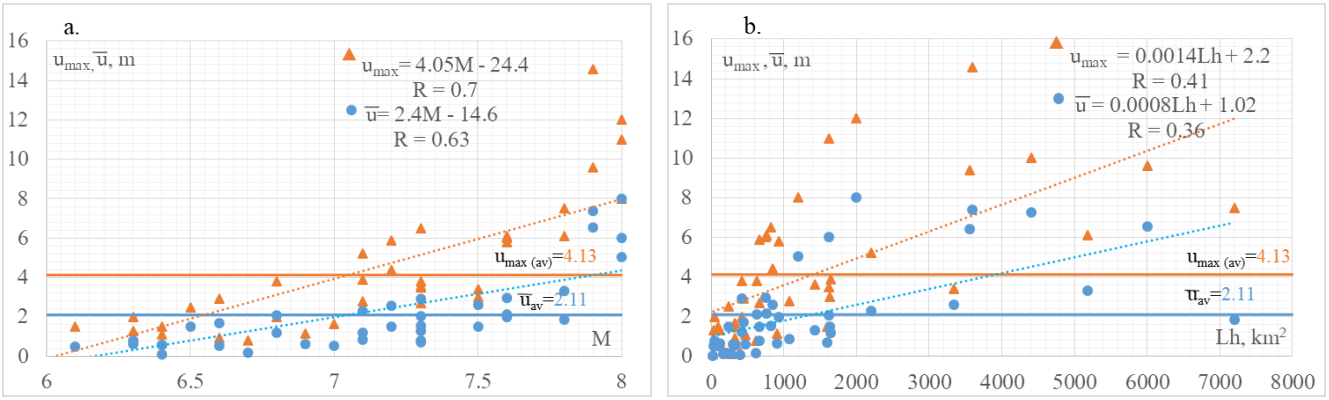

Figure 5. *Dependence of maximum slip u_{max} and mean slip $\overline{u}$ values on: (a) earthquake magnitude M, and (b) on rupture area Lh.*

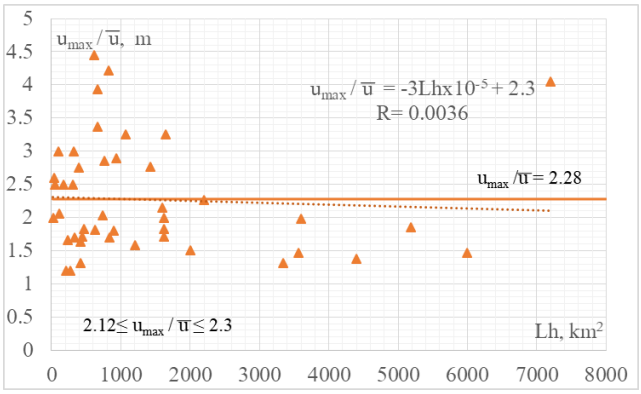

Figure 6. *The dependence of the $u_{max}/\overline{u}$ ratio on the rupture area Lh.*

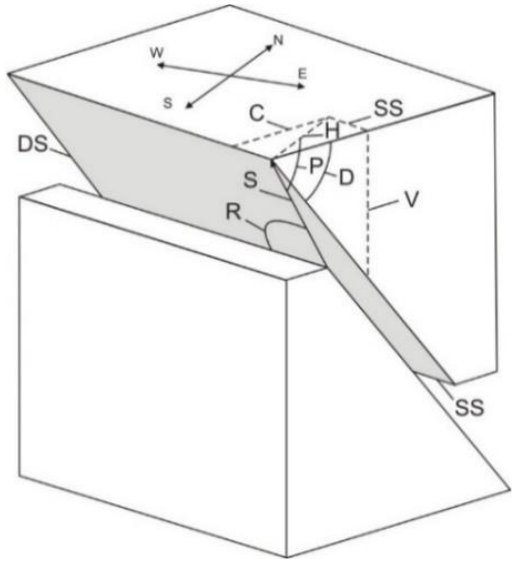

Figure 7. *The diagram of surface rupture formation during the Spitak earthquake [15].*

4. The Energy of the Earthquake with Complex Structure of the Surface Rupture

The formula (1) was derived considering only one component of slip along the rupture. Table 1 column "Type of slip" indicates that some earthquakes had a complex kinematics of the slip, and therefore, energy values obtained for these earthquakes by formula (1) would be the smallest.

This is apparent in the example of the Spitak earthquake of December 7, 1988, the diagram of surface rupture formation of which is presented on Figure 7 [15]. The diagram shows that the earthquake had a right-lateral slip R-RL. The horizontal component of the slip was right-lateral with maximum of $u_{SS} = SS = 0.5M$ measured on-site after the earthquake. Other parameters of this 38 km long rupture were as follows: displacement - $S = 2$ m (measured on-site after the earthquake), vertical component - $V = 2\cos 109^0 = 1.6$ m, compression component - $C = 2\cos 109^0 = 1.1$ m, horizontal component $H = \sqrt{C^2 + SS^2} = 1.2$ m, R=109^0, P=53^0.

In the article [1] the Spitak earthquake energy is calculated by the formula (1) with: $L = 38$ km, $h = 11$ km, $u_{max} = 2$ m, $\overline{u} = 1.22$ m, $R = 10^3(5\overline{u} + 15) = 21.1$ km, and the obtained result is $E_d = 0.45 \cdot 10^{22}$ erg. Similar to [1], let us assume that the average horizontal slip $\overline{u}_{SS}$ would be $\overline{u}_{SS} = u_{ssmax} \times \overline{u}/u_{max} = 0.5 \cdot 1.22/2 = 0.305$ m, and the distance R_{SS} in this case, according to formula (2) would be:

$R_{SS} = 10^3(5 \cdot 0.305 + 15) = 16.52$ km. Since the other parameters would not change, the energy for Spitak earthquake based on formula (1), considering only the horizontal slip would be:

$$E_{SSd} = 0.45 \cdot 10^{22} \frac{\overline{u}_{SS}^2 R}{\overline{u}^2 R_{SS}} = 0.45 \cdot \frac{(0.305)^2 \cdot 21.1}{(1.22)^2 \cdot 16.52} \cdot 10^{22} = 0.036 \cdot 10^{22} erg$$

Thus, the total deformation energy of the Spitak earthquake,

considering the peculiarities of the R-RL rupture would be:

$$E_{ds} = (E_d + E_{Ssd}) = (0.45 + 0.036) \cdot 10^{22} = 0.486 \cdot 10^{22} \text{ erg},$$

$$k_d = \lg(0.486 \cdot 10^{22}) - 7 = 22 - 0.313 - 7 = 14.68$$

That is 8% (or 1.08 times) higher that the value without taking into account the horizontal component of the slip SS=0.5 m. Without the component RL, the energy class of the Spitak earthquake is equal to: $k_d = 14.65$ [1]. The difference of energy classes would be: 14.68-14.65=0.03

5. Strong Earthquake Deformation Areas, Area Locations on Earth's Surface and Aftershock Epicenter Locations

The aftershock process that begins in the post-seismic period is caused by the existence of some deformation energy in the medium outside the rupture zone. The field of accumulated deformations (strains) before the earthquake usually has a very complex structure, related to the non-uniform distribution of rigidity and density characteristics of the rocks, existing fractures and ruptures from the previously occurred earthquakes. That is why the main shock may trigger aftershocks (in the weakened structures) which will last until a new equilibrium is established in the whole medium that was deformed in the pre-seismic period. It is naturally expected that aftershock sources would be located along the line of the main rupture and around it, where strains are already concentrated. Mogi [12] contends that the non-uniform medium in the hypocenter area and minor fractures in it are among the reasons for aftershocks of strong earthquakes, and that a large number of foreshocks and aftershocks indicate that there are many areas with weakened rocks in the medium surrounding the main rupture. According to Kasahara [10], aftershocks and surface deformations tend to be located in the same area around the epicenter.

In the context of the significant deformations area, it means that that aftershocks of the above-mentioned 44 earthquakes should be located within an area 2RL (cm^2):

$$Q_1 = 2RL = 10^{11}L(\overline{u} + 3), \quad (15)$$

where the rupture length L and $(\overline{u} + 3)$ are measured in cm. Actually, as it can be seen on Figure 2c, formula (15) is the sum of slip deformation areas on two sides of the rupture on Earth's surface.

Kasahara [10] presents the following empirical dependence between the area of the epicenter locations of earthquake aftershocks Q_2 (in cm^2) and the magnitude of the main earthquake's shock *M*:

$$\lg Q_2 = 1.02M + 6.0. \quad (16)$$

It is interesting to compare the location area value by formula (16) and the area by the above proposed formula (15). Incidentally, Kasahara [10] also brings up Dambara's [11] formula for determining the radius of the circular area of slip deformations on the surface around the epicenter:

$$\lg r = 0.51M + 2.73, \quad (17)$$

where *r* is the radius of the deformation area measured in cm.

Comparing formula (16) and (17) Kasahara concluded that aftershocks and surface deformations tend to be located in the same plane around the epicenter. Indeed, the area of a circle with the radius *r* equals to $Q_3 = \pi r^2$, and hence:

$$\lg Q_3 = \lg \pi + 2 \lg r, \quad (18)$$

If $\lg r$ from formula (17) is inserted in (18) the following will be derived:

$$\lg Q_3 = 0.496 + 2(0.51\text{M} + 2.73) = 1.02\text{M} + 5.96 \quad (19)$$

which is almost the same as the formula (16).

Thus, in both cases the deformation areas around the earthquake focus are assumed as the aftershocks distribution area. However, it has to be noted that in formula (16) such area corresponds to the earthquake model with a single-point focus, which currently is considered unrealistic, especially for strong earthquakes. "From a physics perspective it is hard to believe that a single point in the rocks can accumulate so much energy and release it instantly. It is then natural to assume that energy processes in the focus are related to some finite volume in Earth" [10]. The above-mentioned model in [1] assumes that the energy release source is a 3D space (Figure 2a) with dimensions L as the rupture length on surface, h as the depth of the earthquake focus and $2R$ as the medium deformation width in the direction perpendicular to the to rupture, depending on the relative deformation (slip) $\bar{u}$ at the rupture. Figure 8 shows the empirical dependence of the deformation energy class value k_d for strong earthquakes with the magnitude $5.6 \leq M \leq 8.5$ on the rupture area Lh, deformation volume $V = 2RLh$ and earthquake's seismic moment M_0.

Figure 8 demonstrates that for earthquake magnitudes $M = 8.0 - 8.5$ the volume of such source could be over 500000 km^3, and the rupture area up to 6000 km^2.

For a comparative analysis, values of Q_1 and Q_2 were calculated by formulas (15) and (16) for 27 earthquakes with magnitudes $M \geq 7.0$, which had high probability of causing a rupture on Earth's surface. Table 2 indicates the parameters of these 27 earthquakes with magnitudes $M \geq 7.0$ and respective values of Q_1, Q_2 ΔQ, $\frac{\Delta Q \cdot 100}{Q_2}$ and Q_1/Q_2. Figure 9 shows the distribution of differences $\Delta Q = Q_1 - Q_2$ in percentages relative to Q_2 for all 27 earthquakes. It can be seen from Table 2 and Figure 9 that the largest difference between Q_1 and Q_2 is observed for four earthquakes: Nos. 5, 14, 16, 19 the rupture

lengths of which are quite big;

$L = 432, 300, 110\ and\ 257$, respectively, while the average slip $\bar{u}$ is relatively small: $\overline{u} = 3.3, 6.54, 2.3$ and 2.6 meters, respectively.

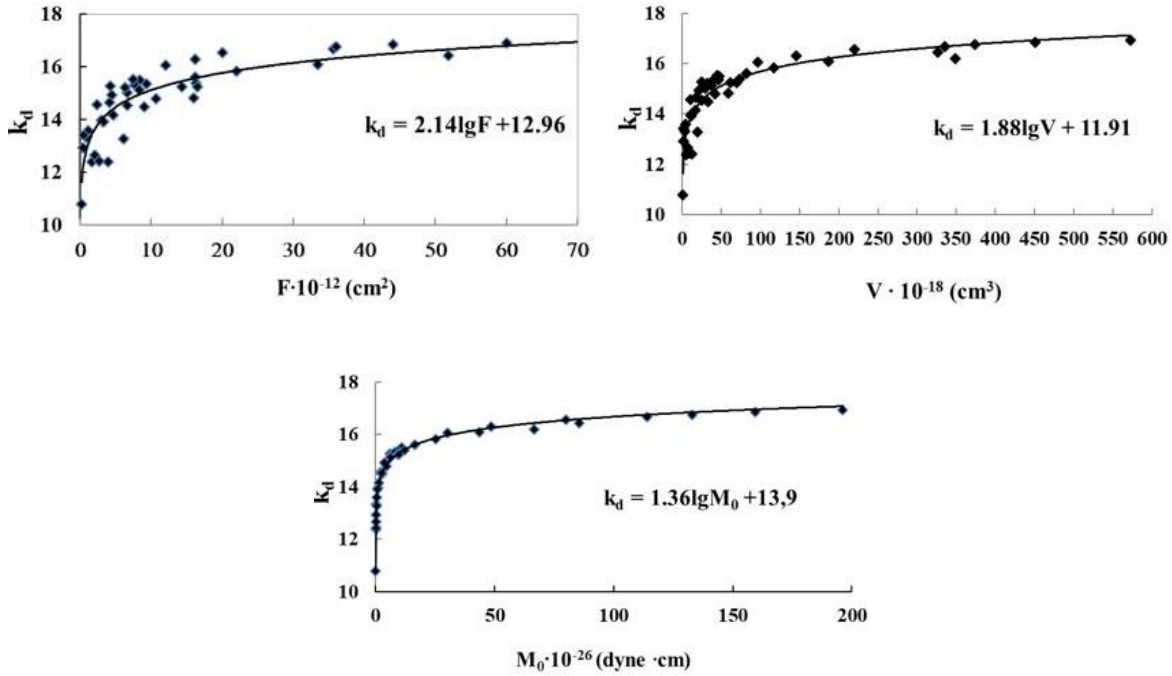

Figure 8. *Dependence of the deformation energy class value* k_d, $(E_d = 10^{k_d})$ *for 44 strong earthquakes with the magnitude* $5.6 \leq M \leq 8.5$ *on the rupture area* $F = Lh$, *deformation volume* $V = 2RLh$ *and earthquake's seismic moment* M_0.

Table 2. *Earthquake parameters and comparison of the aftershock areas based on formulas (15) and (16) for 27 earthquakes with magnitudes M≥7.0 [8].*

No. earthquake	Country	Earthquake location	Date of the earthquake	Earthquake Magnitude M_s	Length of the gap L (km)	Depth of the rupture h (km)	Maximum movement u_{max} (m)	Average movement $\bar{u}$ (m)
1	USA	Fort Tejon	09.01.1857	8.3	297	12	9.4	6.4
2	USA	Owens Valley	26.03.1872	8	108	15	11	6
3	Japan	Nobi	27.10.1891	8	80	15	8	5.04
4	Japan	Rikuu	31.08.1896	7.2	40	21	4.4	2.59
5	USA	San Francisco	1/13/1906	7.8	432	12	6.1	3.3
6	USA	Pleasant Valley	10/3/1915	7.6	62	15	5.8	2
7	China	Kansy	12/16/1920	8.5	220	20	10	7.25
8	Japan	North Izu	11/25/1930	7.3	35	12	3.8	2.9
9	China	Kehetuohai	8/10/1931	7.9	180	20	14.6	7.38
10	Turkey	Erzihcan	12/26/1939	7.8	360	20	7.5	1.85
11	USA	Imperial Valley	5/19/1940	7.2	60	11	5.9	1.5
12	China	Damxung	11/18/1951	8	200	10	12	8
13	Turkey	Abant	5/26/1957	7	40	8	1.65	0.55
14	Mongolia	Gobi-Altai	12/4/1957	7.9	300	20	9.6	6.54

No. earthquake	Country	Earthquake location	Date of the earthquake	Earthquake Magnitude M_s	Length of the gap L (km)	Depth of the rupture h (km)	Maximum movement u_{max} (m)	Average movement $\bar{u}$ (m)
15	USA	Hebgen Lake	8/18/1959	7.6	45	17	6.1	2.14
16	Iran	Dasht-e-Bayaz	8/31/1968	7.1	110	20	5.2	2.3
17	Turkey	Gediz	3/28/1970	7.1	63	17	2.8	0.86
18	China	Luhuo	2/6/1973	7.3	110	13	3.6	1.3
19	Guatemala	Motagua	2/4/1976	7.5	257	13	3.4	2.6
20	Turkey	Caldiran	11/24/1976	7.3	90	18	3.5	2.05
21	Iran	Tabas-e-Colshan	9/16/1978	7.5	74	22	3	1.5
22	Iran	Koli	11/27/1979	7.1	75	22	3.9	1.2
23	Algeria	El Asman	10/10/1980	7.3	55	15	6.5	1.54
24	USA	Borah Peak	10/28/1983	7.3	33	20	2.7	0.8
25	Armenia	Spitak	12/7/1988	7	38	11	2	1.22
26	China	Lancand Gengma	11/6/1988	7.3	80	20	1.5	0.7
27	USA	Landers	6/28/1992	7.6	62	12	6	2.95

Table 2. *Contiuned.*

No. earthquake	The value of R according to the formula (2) (km)	Size of the area $Q_1/10^{14}$, to the formula (15), cm^2	Size of the area $Q_2/10^{14}$, to the formula (16), cm^2	Difference in areas Q_1-Q_2=$\Delta Q/10^{14}$, cm^2	Deviations $\Delta Q/Q_2$ in %	Deviations Q_1/Q_2
1	47	3.02	2.92	0.10	3.42	1.03
2	45	0.97	1.45	-0.48	-33.10	0.67
3	40.25	0.64	1.45	-0.81	-55.86	0.44
4	27.95	0.22	0.22	0.00	0.00	1.00
5	31.5	2.72	0.90	1.82	202	3.02
6	25	0.31	0.56	-0.25	-44.64	0.55
7	51.25	2.26	4.68	-2.42	-51.71	0.48
8	29.5	0.21	0.28	-0.07	-25.00	0.75
9	51.9	1.87	1.14	0.73	64.04	1.64
10	24.25	1.75	0.90	0.85	94.44	1.94
11	22.5	0.27	0.22	0.05	22.73	1.23
12	65	2.60	1.45	1.15	79.31	1.79
13	17.75	0.14	0.14	0.00	0.00	1.00
14	47.7	2.86	1.14	1.72	151	2.51
15	25.7	0.23	0.56	-0.33	-58.93	0.41
16	26.5	0.58	0.17	0.41	241	3.41
17	19.3	0.24	0.17	0.07	41.18	1.41
18	21.5	0.47	0.28	0.19	67.86	1.68

No. earthquake	The value of R according to the formula (2) (km)	Size of the area $Q_1/10^{14}$, to the formula (15), cm^2	Size of the area $Q_2/10^{14}$, to the formula (16), cm^2	Difference in areas Q_1-Q_2=$\Delta Q/10^{14}$, cm^2	Deviations $\Delta Q/Q_2$ in %	Deviations Q_1/Q_2
19	28	1.44	0.45	0.99	220	3.20
20	25.25	0.45	0.28	0.17	60.71	1.61
21	22.5	0.33	0.45	-0.12	-26.67	0.73
22	21	0.32	0.17	0.15	88.24	1.88
23	22.7	0.25	0.28	-0.03	-10.71	0.89
24	19	0.13	0.28	-0.15	-54	0.46
25	21.1	0.16	0.14	0.02	14.29	1.14
26	18.5	0.30	0.28	0.02	7.14	1.07
27	29.75	0.37	0.56	-0.19	-33.93	0.66
Average value					36	1.36
Average value without earthquakes № 5, 14, 16, 19					6.49	1.06

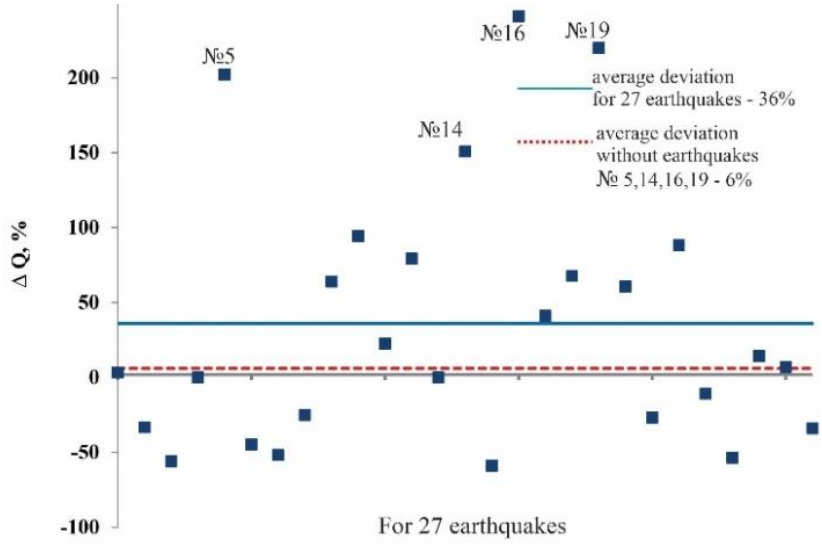

Figure 9. *Dependence of aftershock location area differences in percent between formula (16) and empirical formula (15) for 27 earthquakes with magnitudes* $M \geq 7.0$.

If these four earthquakes are excluded as "unusual", the mean values of percentage differences of $\Delta Q$and area ratio differences Q_1/Q_2 would amount at 6% and 1.06 times, respectively.

Figure 10 shows logarithmic and linear dependencies of aftershock location areas Q_1, Q_2on magnitudes $M \geq 7.0$ for 23 strong earthquakes.

Logarithmic dependencies are:

$$lg\ Q_1 = 0.83M + 7.36$$

$$lg\ Q_2 = 1.02M + 6.0 \qquad (19)$$

Linear dependencies are:

$$Q_1 \times 10^{-14} = 1.82M - 12.8$$

$$Q_2 \times 10^{-14} = 2.21M - 15.9 \qquad (20)$$

Let us use the example of Spitak earthquake with $M = 7.0$, $L = 38$ km, $\overline{u} = 1.22$ m, $R = 21.1$ km, to calculate aftershock location areas using different methods.

Based on the empirical formula (16):

$$lg\ Q_2 = 1.02 \cdot M + 60 = 1.02 \cdot 7.0 + 6 = 13.14$$

$$Q_2 = 10^{13.14} cm^2 = 0.138 \cdot 10^{14} \approx 0.14 \cdot 10^{14} cm^2$$

Based on the proposed formula (15):

$$Q_1 = 10^{11} L(\bar{u} + 3)$$

$$Q_1 = 10^{11} \cdot 38(1.22 + 3) = 0.16 \cdot 10^{14} cm^2$$

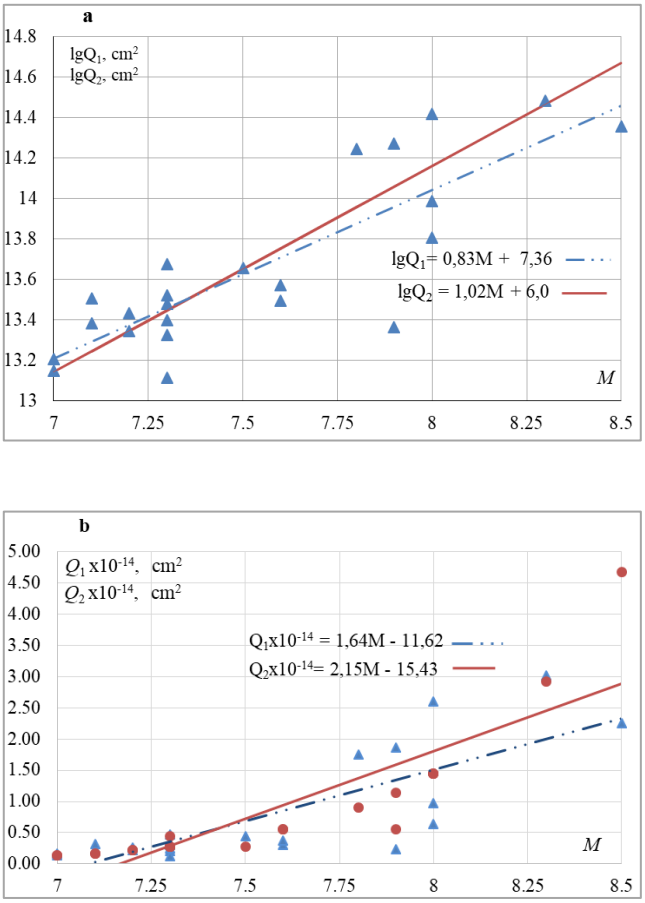

Figure 10. *Logarithmic and linear dependencies of aftershock location areas Q_1 and Q_2 on earthquake magnitude M, based on formulas (15) and (16).*

Now let us calculate the actual area Q_r of aftershock locations after the Spitak earthquake. According to [9], the Spitak earthquake had over 200 aftershocks with $1 < M < 4.5$, the map of locations of which is provided in Figure 11 [9], where the nominal dotted rectangle having sides with lengths of 52.2 km and 32.1 km is used to calculate their area. The actual area Q_r is then (Figure 11):

$$Q_r = 53.6 \cdot 32.1 = 1720.56\ km^2 = 0.17 \cdot 10^{14} cm^2$$

Apparently the differences between the values Q_1, Q_2 and Q_r are insignificant and they can be assumed acceptable to solve such seismology problems, as determining the earthquake aftershocks area. It follows from these data that for the majority of usual earthquakes, formulas (15) and (16) are well correlated for determining the area of aftershocks epicenter locations, and for the Spitak earthquake Q_r turned to be closer to Q_1.

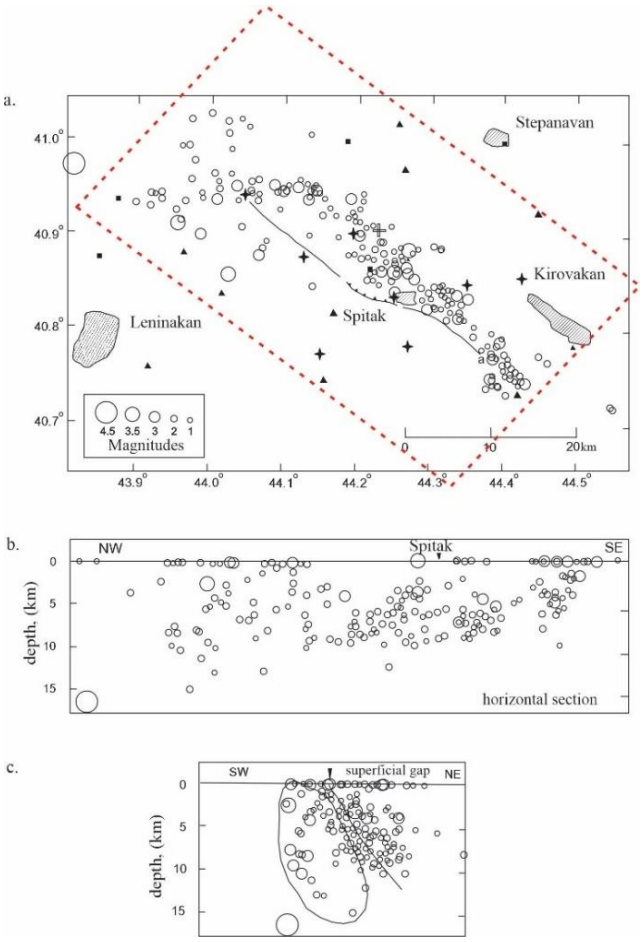

Figure 11. *Locations of aftershock epicenters of Spitak earthquake 7.12.1988 [9] and the nominal rectangle (dotted) of calculated aftershocks area. a. geographic location of epicenters b. Projection of hypocenters on the plane of the rupture, c. hypocenters in the zone of the plane perpendicular to the surface [9].*

It has been shown that areas of aftershocks and deformations around the rupture on Earth's surface are identical, and their area can be determined using the values of rupture length L and mean slip $\bar{u}$ at the rupture after the earthquake.

New empirical logarithmic and linear relations were determined between the strong earthquake's aftershock locations area and the magnitude of the main shock.

6. Main Results of Works 1, 2, 3, 4

1. A new model is proposed from the point of view of mechanics of solid mechanical bodies, the occurrence and origin of a strong earthquake based on quantitative real deformation parameters of the consequences of earthquakes on the earth's surface: the length of the rupture, the depth of the source and the relative move-

ment along the line of extension of the new rupture.

2. On this basis, a new method has been developed for determining the magnitude of earthquake energy, the ultimate shear deformation of the earth's crust, the spatial dimensions of the focal zone (where the mechanical potential energy of the deformed medium of the earth's crust slowly accumulates, stresses relieved after an earthquake (Reid's Hypothesis), the areas of the deformed medium of the earth's surface and the location of aftershocks on the earth's surface and predicting the values of seismograms and accelerograms for future strong earthquakes.
3. Numerous new empirical relationships have been established between different levels of earthquake consequences and its force elements: magnitude, seismic moment, accelerations, velocities and displacements.
4. Based on the above studies, a new method has been developed for reliable prediction of seismograms, velisograms and accelerograms and their change over time, shear deformations of soils along the depth of the foundation during strong earthquakes depending on the magnitude of the predicted earthquake, soil conditions of the construction site and the distance before the rupture of the predicted earthquake on the earth's surface: It is shown that the spectra of earthquake reactions obtained on the basis of synthetic accelerograms are both quantitatively and qualitatively close to the spectra of reactions obtained on real accelerograms of strong earthquakes. The main positive result of these studies is that they indicate the possibility of using synthetic accelerograms and seismograms in assessing the degree of seismic hazard of territories, ensuring seismic safety of especially important objects and underground structures, as well as in scientific research on improving the method of calculating buildings and structures for seismic impacts.

Author Contributions

Eduard Khachiyan is the sole author. The author read and approved the final manuscript.

Conflicts of Interest

The authors declare no conflicts of interest.

References

[1] Khachiyan E. Y., Method for determining the potential strain energy stored in the earth before a large earthquake. Science Publishing Group, Earth Sciences, 2013, 10(2), pp. 47-57., https://doi.org/116448/j.earth.20130202.14

[2] Khachiyan E. Y., On determining of the ultimate strain of earth crust rocks by the value of relative slips on the earth surface after a large earthquake. Science Publishing Group, Earth Sciences, 2016, 5, pp. 111-118, https://doi.org/10.11648/j.earth.20160506.14

[3] Khachiyan E. Y., Predicting of the seismogram and accelerogram of strong motions of the soil for an earthquake model considered as an instantaneous rupture of the earth's surface. Science Publishing Group, Earth Sciences, 2018, 7, pp. 183-201. https://doi.org/10.11648/j.earth.20180704.16

[4] Khachiyan E. Y., Analysis of the Values of Ground Displacements, Shear Strains, Velocities and Accelerations, and Response Spectra of Strong Earthquake by Synthetic Accelerograms. Science Publishing Group, Earth Sciences, 2022, 11(5), pp. 327-337, https://doi.org/10.11648/j.earth.20221105.19

[5] Brune J. N., Seismic Risk and Engineering Decisions, The Physics of Earthquake Strong Motion, in Lomnitz C. and Rosenblueth E., Eds., New York: Elsevier Sci. Publ. Co., 1976, pp. 141-177.

[6] Aki K. Generation and propagation of G waives from the Niigata Earthquake of June, 16, 1964, Estimation of Earthquake moment, Released energy, and stress –strain drop from G wave spectrum. Bull. Earthquake Res. Inst., Tokyo Univ., 1966, 44: 73-88.

[7] Timoshenko S., Gere J. Mechanics of Materials, New York, Nan Nostrand Renhold Company, 1972, P. 669.

[8] Wells D. L., and Coppersmith K. I., New Empirical Rela¬tionship among Magnitude, Rupture Length, Rupture Width, Rupture Area, and Surface Displacement, Bull. Seismol. Soc. Amer., 1994, vol. 84, no. 4, pp. 974-1002.

[9] Cisternas A., Philip H., Bousquet J. C., Cara M., Deschamps A., Dorbath L., Dorbath C., Haessler H., Jimenez E., Nercessian A., Rivera L., Romanowicz B., Gvishiani A., Shebalin N. V., Aptekman I., Arefiev S., Borisov B. A., Gorshkov A., Graizer V., Lander A., Pletnev K., Rogozhin A. I., Tatevossian R. The Spitak (Armenia) earthquake of 7 December 1988: field observations, seismology and tectonics // Nature. 1989. V. 339. P. 675–679. https://doi.org/10.1038/339675a0

[10] Kasahara K. Earthquake Mechanics, Cambridge University Press, 1981, P. 263.

[11] Dambara T. A revised relation between the area of the crustal deformation associated with an earthquake and its magnitude // Rep. Coord. Comm. Earthq. Predict. 1979. V. 21. P. 167–169. [in Japanese].

[12] Mogi K. Earthquake Prediction, Academic Press, 1985, P. 382.

[13] Rikitake T. Earthquake Prediction. Elsevier Scientific Publishing. Amsterdam, 1976, P. 357.

[14] Khachiyan E. Y. On a Simple Method for Determining the Potential Strain Energy Stored in the Earth before a Large Earthquake. Journal of Volcanology and Seismology, 2011, Vol. 5, No. 4, pp. 286-297. Pleiades Publishing, Ltd., 2011, https://doi.org/10.11.34/s0742046311040038

[15] Sharp R. V. Surface Faulting: A preliminary view. Earthquake Spectra. The Professional Journal of the Earthquake Engineering Institute, USA, Special Supplement, Armenia Earthquake Reconnaissance Report, August 1989, pp. 13-22.

Biography

Eduard Khachiyan Was born 17.08.1933. Khachiyan extensive academic and research career includes roles at the Armenian Earthquake Engineering Research Institute (1956-2002), the American University of Armenia (1992-1997), and since 1997, he has served as head of the Chair of Building Mechanics at Yerevan State University of Architecture and Construction and chief scientist at the Institute of Geological Sciences of Armenia. His research focuses on applied seismology, earthquake engineering, dynamics of structures, and building mechanics. Khachiyan has authored over 290 scientific papers and received numerous accolades. His recent works include publications in Erath Sciences, Seismic Instruments and Novel Perspectives of Engineering Research. Any other remarkable point (s): Building Norms of RA II-2.02-94, II-6.02-2006, II-20.04-2020 "Earthquake engineering. Design standards" Yerevan 1994, 2006, 2020. Participation in the projects of research works primary design and re-application of the Armenian nuclear power plant.

Research Field

Eduard Khachiyan: Applied seismology, Earthquake engineering, Dynamic of Structures, Building mechanics, Design standards, Seismic effects and Prognosis of structures behavior.